CHARGE STRIPPER AND MEBT FOR THE ^{3}He RFQ ACCELERATOR*

F. M. Bieniosek, K. Anderson, R. J. Pasquinelli, M. Popovic, C. W. Schmidt and R. Webber
Fermilab, Batavia, IL 60510 USA*
D.J. Larson and P. Young
SAIC, 4161 Campus Point Ct., San Diego, CA 92121

Abstract

The ^{3}He RFQ linac for production of positron-emitting radioactive isotopes accelerates singly-ionized $^3He^+$ ions to an energy of 1 MeV in a 212.5-MHz RFQ. The ions are then stripped to form doubly-ionized $^3He^{++}$ in a gas-jet stripping cell, and transported by the MEBT to the 425-MHz RFQ string for acceleration to 10.5 MeV. The stripper cell utilizes a mechanical injector to provide gas pulses to a nozzle. The directed gas jet passes across the beam into a scavenge section which pumps away the gas. The MEBT is an achromatic, isochronous transport section based on two 270-degree bend magnets. It provides bunched and focused beam to the 425-MHz RFQ string.

INTRODUCTION

A Fermilab/SAIC collaboration has been developing a ^{3}He RFQ accelerator for production of positron-emitting isotopes for positron emission tomography (PET).[1] The accelerator consists of a $^3He^+$ ion source, a low-energy beam transport (LEBT) line, a 212.5-MHz radio-frequency quadrupole (RFQ) to accelerate $^3He^+$ to 1 MeV, a gas stripping cell, a medium-energy beam transport (MEBT) line, a string of three 425-MHz RFQs to accelerate $^3He^{++}$ to 10.5 MeV, and a high-energy beam transport (HEBT) line to the target. The beam is produced in macropulses of up to 70 μs long, at up to 360-Hz repetition rate. The ion source produces about 25 mA (peak) of singly-ionized ^{3}He. At low energy a doubly-ionized $^3He^{++}$ beam ions is difficult to generate in a nonplasma stripper because of charge-exchange processes. The approach taken to produce a $^3He^{++}$ beam is to accelerate the $^3He^+$ beam to 1 MeV in the 212.5-MHz RFQ. At this energy, a stripping efficiency in the range of 80% can be achieved in a gas stripping cell. At an energy of 1 MeV and an average current of several hundred μA, carbon foil strippers are not expected to survive the high power density. In the stripper cell and beyond, the beam rapidly debunches due to the large (1.7%) velocity spread coming out of the RFQ. As a result the beam must be rebunched. Initially the accelerator utilized an RF buncher to rebunch the beam. Difficulties were encountered in operation of this device, probably due to the large number of free electrons streaming from the gas stripper cell. Thus the MEBT was designed to be a purely magnetic achromatic, isochronous beam line. Free electrons from the stripper cell no longer have a deleterious effect on operation of the MEBT, and may in fact be necessary for its efficient operation. Details of the MEBT design are presented in a companion paper [2].

CHARGE STRIPPER

A gas-jet stripper was chosen, rather than a differentially-pumped gas cell, for the following reasons.

1. It is desirable to maintain pressure in the RFQ and the MEBT as low as possible. Because the gas is flowing in a jet the pressure for a given gas density in the stripping region is much lower than for a static fill. Thus it is easier to keep the stripper gas out of the RFQ and MEBT.
2. Expectations are that a static-filled cell will suffer from significant beam heating of the gas. As a result the gas density may vary during the pulse as the gas is heated. Thus the pressure in a cell would have to be increased from that sufficient to strip a low intensity beam.
3. By operating with a pulsed gas jet synchronized with the beam it is possible to further reduce the gas load on the stripper pump.

An automotive-type fuel injector (Nissan) provides gas pulses to a converging-diverging nozzle. The injector provides average gas flow rates in excess of 12 Torr-liter/sec in pulses of 300-500 μs duration at up to 360 Hz. A MOSFET-based pulser delivers 75 V, 200-300 μs pulses to the injector. A directed gas jet of line density approximately 3-6 x 10^{16} cm^{-2} is created at the nozzle. It passes across the beam and is directed into the scavenge section. The flow rate of the gas is sufficient to prevent excessive heating of the gas by the beam. A significant fraction of the injected gas is pumped away between beam pulses.

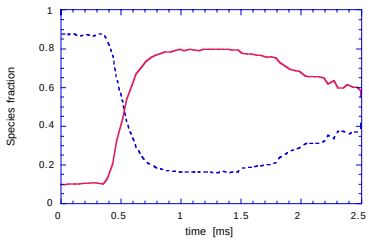

Figure 1. Yield of He^+ (dashed) and He^{++} (solid) beam in the Faraday collectors as a function of stripper delay time in the prototype stripper cell for argon gas at 60 Hz.

A prototype stripper cell was built to determine efficiency and gas flow in a realistic geometry. Total pumping capacity in the prototype cell was 1000 Torr liter/sec. A

* Operated by the Universities Research Association Inc., under contract with the U.S. Department of Energy.

0-7803-4376-X/98/$10.00 © 1998 IEEE

magnetic spectrometer that bends the 1-MeV He^+ and He^{++} beam ions into Faraday collectors at bend angles of 11.5° and 23.6° respectively, was used to test operation of the gas jet. Stripping efficiency was determined by measuring the relative distribution of beam current on the two collectors. Typical performance is shown in Figure 1. Under these conditions (argon gas at 60 Hz), the pressures were about 3 mTorr in the stripper turbo region, about 2 mTorr in the stripper top section, and 2.5 μTorr in the RFQ. The stripper cell was analytically modeled by calculating aperture conductances throughout the stripper and incorporating these numbers into an ANSYS finite-element model. The measured operating pressures were in agreement with predictions from the model. Several gases were tested in the prototype cell: Ar, N_2, Kr, CO_2, and He in order of decreasing stripping efficiency. The best stripping efficiency was obtained with argon gas, reaching over 80%.

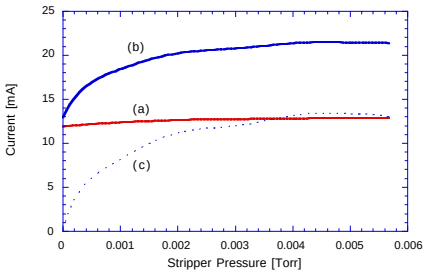

Figure 2. Current through MEBT toroids as a function of stripper pressure for nitrogen gas at 360 Hz, (a) before stripper, (b) after stripper, (c) at end of MEBT.

Based on the successful operation of the prototype stripper cell, an operational version was constructed. This stripper cell differs from the prototype cell mainly in increased pumping capacity. Pumping capacity is 1000 Torr-liter/sec at the stripper outer housing (behind the nozzle), and 3000 Torr-liter/sec at the scavenge section facing the nozzle. The nozzle is an converging-diverging nozzle with a 0.5-mm diameter throat. Typical operating pressures are 3.4 mTorr at the scavenge section, 0.8 mTorr at the stripper outer housing, 19 μTorr in the MEBT, and 0.7 μTorr in the RFQ. Typical results are shown in Figure 2 for 360 Hz operation in nitrogen gas. The curve was generated by varying the length of the electrical pulse delivered to the injector in the stripper. As the pulse is lengthened, the amount of gas delivered per pulse increases up to a limit determined by the injector. As the amount of gas increases, the signal in the toroid before the stripper increases due to the presence of electrons streaming out of the stripper cell toward the RFQ. Electron currents are also detected in the toroid after the stripper. Significant electron currents are not observed in the toroid at the end of the MEBT. Slightly higher stripping efficiency can be obtained in argon gas. The vacuum turbopumps, however, have some difficulty pumping argon because of the high molecular weight and low thermal conductivity, causing excessive heating and slowing down of the vanes. As a result the stripper cell utilizes nitrogen gas in normal operation. To date, electrical beam currents of up to 21 mA have been observed at the end of the MEBT.

Measurements of beam profile by scanning the beam across a single wire were made before and after stripping the beam in the prototype spectrometer chamber. No measurable beam size increase, implying negligible emittance growth, was observed. A general calculation of the small-angle multiple scattering of ions in a gas target can be found in [3].

MEBT

The MEBT was designed to transport and match the beam to the 425-MHz RFQ string, focused to a small spot transversely, and with minimum longitudinal extent. It was instrumented for commissioning by:

a. current-monitor toroids located before the stripper, after the stripper, and at the end of the MEBT,
b. multi-wire profile monitors at the entrance and exit of the first 270° magnet, at the entrance of the second 270° magnet, and at the end of the MEBT,
c. an emittance scanner at the end of the MEBT for emittance measurements, and
d. electron suppressers in the cross-over arm.
e. At the conclusion of low-intensity MEBT commissioning, the profile monitors were removed and replaced by Faraday aperture plates, which were designed to skim the edges of the beam, providing a minimally intercepting measure of beam position in the MEBT.

The profile monitors were used to measure the beam size at various locations, and to ensure that the MEBT was symmetrical in operation. The emittance scanner was used to verify that the emittance growth through the MEBT was negligible. It was found that the measured horizontal emittance was a sensitive function of trim quad settings, which control dispersion. Dispersion results in increased beam size at the end of the MEBT. Zeroing the dispersion by adjusting the trim quads and moving magnets in the return leg of the MEBT minimized the horizontal emittance. Final emittance measurements in both planes showed no significant emittance growth. At completion of commissioning the stripper/MEBT combination had a typical efficiency of 65%, in line with expectations. Before commissioning of the MEBT, it was postulated that space-charge effects might significantly impact tuning of the MEBT. Typical variations in field strengths of MEBT quads due to space charge were predicted to be in the range of 10-20%. An additional concern was emittance growth driven by nonlinear space-charge. In fact, little effect of space charge was noted. No significant change in MEBT tune was observed with beam intensity, and the electron suppresser electrodes had no significant effect. This result is attributed to either charge neutralization by electrons or spreading and reduced beam density in the MEBT. There are numerous sources of electrons available to supply charge neutralization:

1. In the stripper, one free electron is produced per stripped 1 MeV He^+ beam ion with an electron energy of 180 eV.
2. Ionization of the stripper gas by the beam produces electrons more numerous than beam electrons by a

factor of 3 to 10, because the ionization cross section of stripper gas is typically much larger than for beam ions. These electrons are born with a temperature of about 30 eV [4]. Secondary electrons are also produced by collisions between energetic electrons with gas molecules.

3. In the balance of the MEBT, some electrons produced in the stripper are transported downstream with the beam. Electrons are also produced locally by beam ions on background gas, and by beam ions scraping on the vacuum wall.

One limitation to performance of the MEBT is the curvature in the bends. For example, the longitudinal velocity of the neutralizing electrons leads to a centrifugal force on the electron due to the curvature around the bend. A radial (horizontal) electric field must arise to balance this force. The electric field comes from a shift in the electron distribution radially (horizontally) outward from the centroid of the beam path. An estimate of the electric field may be determined by equating the two forces. The force is $F = mv^2/\rho = eE$, or $E = 2 *$ kinetic energy / $e\rho$. The kinetic energy of the electrons is likely to be less than 30 eV. Using this value, and the radius of curvature ρ = 30 cm, the electric field is E = 2 V/cm. This electric field is transverse to the beam in the horizontal direction. Since it is not symmetric, it may cause some distortion of the beam. However, it is small enough to not be a concern in the present case.

The beam is clearly bunched as it leaves the MEBT. Bunched beams were seen on a fast oscilloscope, and scaling of the profile was quantitatively measured on a spectrum analyzer viewing signals on a wire that intercepts the beam.

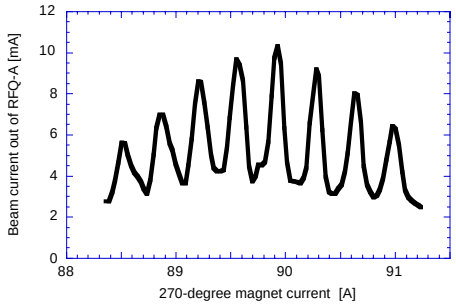

Figure 3. Current from RFQ-A as a function of 270° magnet current, with phase feedback loop off.

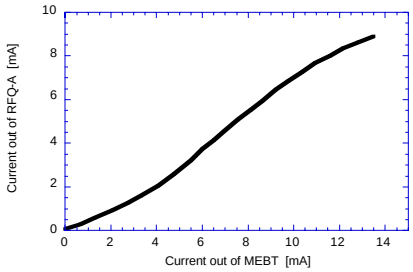

Figure 4. Beam current from RFQ-A as a function of beam current from MEBT at 30 Hz.

Measurements of transmission through the first RFQ in the 425-MHz string (RFQ-A) are indicated in Figures 3 and 4. Figure 3 shows the transmission through RFQ-A as a function of the 270° magnet current. Both 270° magnets are driven by the same power supply. The oscillatory nature of the transmission curve is due a change in the path length through the MEBT as the radius of curvature of the beam in the 270° magnet varies. When the path length is such that the difference in phase between the 212-MHz RFQ and RFQ-A is $2\pi m$, where m is an integer, the beam enters RFQ-A in phase, and it is accelerated. When the path length is changed such that the beam enters out of phase, it is not accelerated. With further changes in the path length the cycle repeats. The path length through the 270° magnets is $3\pi\rho$ where the radius of curvature on axis is ρ = 30.48 cm. The length corresponding to 360 degrees of rf phase at 425 Mhz is $\lambda = \beta c/f = 0.0267 \cdot 3 \times 10^{10} / 425 \times 10^{6} = 1.88$ cm. Thus a complete cycle should occur for a relative path-length change of $ds/s = \lambda/3\pi\rho = 0.654\%$. The 270° magnets are in the linear regime, i.e. dB/B = dI/I. Neglecting the field index in the 270° magnets $n = -(\rho/B)\cdot\partial B/\partial r = 0.53$, the relative change in path length for a given change in magnet current is $ds/s = d\rho/\rho = dI/I$, or one cycle in 0.587 A. Taking into account the field index, and the fact that the beam travels 3/4th of a complete turn in each magnet, the relative change in path length for a given change in magnet current is roughly $ds/s = (1+7n/6)\, dI/I$. A complete cycle then should correspond to a current change of 0.36 A. This result agrees well with the measured rate (Figure 3), which is 7 cycles in 2.5 A, or about 0.36 A per cycle. The ratio of in-phase to out-of-phase signal, which is about 3, implies that most of the beam is properly bunched as it enters the RFQ. In order to minimize the sensitivity of accelerator performance to length of the MEBT, under normal operation the low-level rf RFQ drive signal is phase-locked to the beam signal collected on a Faraday aperture plate at the end of the MEBT.

Figure 4 shows the efficiency of acceleration, with only RFQ-A installed after the MEBT, as a function of incident beam current. Nominal beam energy at the exit of RFQ-A is 5 MeV. Typical efficiency is in the range of 60-70%. The variations in incremental efficiency with beam intensity may be due to residual space charge effects in the MEBT, and limitations in rf power in the RFQ. The maximum accelerated beam at 5 MeV observed was over 11 mA. Beam acceleration was verified by placing a 12.7-μm aluminum foil at the exit of the RFQ-A. This thickness of foil passes the 5-MeV He beam ions, but stops any 1-MeV ions. After correcting for electrons produced in the foil, no significant reduction in collected current with the foil in place was noted. At present the accelerated beam through the entire 425-MHz RFQ string (10.5 MeV) is in the range of 6 mA.

[1] R. J. Pasquinelli, *et.al*., A $^3He^{++}$ RFQ Accelerator for the Production of PET Isotopes, Paper 9B9.
[2] D. J. Larson, *et.al*. Ion Optical Design of the BRF-FNAL-SAIC-UW PET Accelerator, Paper 4V18.
[3] P. Sigmund, K. B. Winterbon, Nucl. Instr. Meth. 119, 541 (1974).
[4] M. Reiser, Theory and Design of Charged Particle Beams, Wiley, 1994, p. 4.302.